THE JOURNAL OF BIOLOGICAL CHEMISTRY VOL. 282, NO. 25, pp. 18625–18633, June 22, 2007

Ajulemic Acid, a Synthetic Nonpsychoactive Cannabinoid Acid, Bound to the Ligand Binding Domain of the Human Peroxisome Proliferator-activated Receptor γ*

Received for publication, March 23, 2007, and in revised form, April 16, 2007 Published, JBC Papers in Press, April 26, 2007, DOI 10.1074/jbc.M702538200

Andre L. B. Ambrosio[‡1], Sandra M. G. Dias[§], Igor Polikarpov[‡], Robert B. Zurier[¶], Sumner H. Burstein[‖], and Richard C. Garratt[‡2]

From the [‡]Centro de Biotecnologia Molecular Estrutural, Instituto de Física de São Carlos, Universidade de São Paulo, São Carlos-SP CEP 13560-970, Brazil, the [§]C3-137 Veterinary Medical Center, Cornell University, Ithaca, New York 14853, and the Departments of [¶]Medicine and [‖]Biochemistry and Molecular Pharmacology, University of Massachusetts Medical School, Worcester, Massachusetts 01605

Ajulemic acid (AJA) is a synthetic analog of THC-11-oic acid, a metabolite of tetrahydrocannabinol (THC), the major active ingredient of the recreational drug marijuana derived from the plant *Cannabis sativa*. AJA has potent analgesic and anti-inflammatory activity *in vivo*, but without the psychotropic action of THC. However, its precise mechanism of action remains unknown. Biochemical studies indicate that AJA binds directly and selectively to the isotype γ of the peroxisome proliferator-activated receptor (PPARγ) suggesting that this may be a pharmacologically relevant receptor for this compound and a potential target for drug development in the treatment of pain and inflammation. Here, we report the crystal structure of the ligand binding domain of the γ isotype of human PPAR in complex with ajulemic acid, determined at 2.8-Å resolution. Our results show a binding mode that is compatible with other known partial agonists of PPAR, explaining their moderate activation of the receptor, as well as the structural basis for isotype selectivity, as observed previously *in vitro*. The structure also provides clues to the understanding of partial agonism itself, suggesting a rational approach to the design of molecules capable of activating the receptor at levels that avoid undesirable side effects.

Peroxisome proliferator-activated receptors (PPAR)[3] are members of the nuclear receptor superfamily of ligand-activated transcription factors. Three closely related mammalian isotypes of PPAR, termed α, γ, and δ, which show distinct functions and tissue distributions, have been characterized (1). PPARs act as heterodimers in partnership with the retinoid X receptor-α and, upon binding of an agonist, the complex recognizes specific peroxisome proliferator response elements leading to the transcriptional regulation of target genes.

The γ isotype (PPARγ) in particular is involved in a range of distinct physiological processes including fat cell differentiation, glucose homeostasis, lipid metabolism, aging, and inflammatory and immune responses. For this reason, PPARγ has been identified as a molecular target in the treatment of diseases such as diabetes, dyslipidemia, hypertension, obesity, and in the modulation of the immune and inflammatory responses (2–5). As a consequence, PPARγ is believed to be a key target for development of novel drug-based therapies.

The first crystal structures of the PPARγ ligand binding domain (LBD) revealed a large T-shaped hydrophobic ligand binding cavity, of about 1300 Å^3 in volume (6, 7). This observation explained the ability of this receptor to bind a wide range of both naturally occurring and synthetic substances. Examples of ligands are naturally occurring fatty acid metabolites, including 15-deoxy-$\Delta^{12,14}$-prostaglandin J2 (8, 9) and the products of oxidized low-density lipoprotein, such as 13-hydroxyoctadecadienoic acid and 15-hydroxyeicosatraenoic acid (10). Synthetic ligands of PPARγ include a class of insulin-sensitizing drugs referred to as thiazolidinediones (TZDs) or glitazones (11, 12) and the GW series of L-tyrosine analogs (13). The number of known PPARγ ligands continues to increase.

Novel PPARγ ligands are being discovered, seeking to improve efficacy and tolerability as compared with the currently available agonists (such as the TZDs and GW series) and also aiming toward new therapeutic benefits. Cannabinoids may be included in this group. Cannabinoids are a group of chemicals first identified as a result of their activating effect on the cannabinoid receptors CB1 and CB2. Currently, they can be grouped into three general types: *herbals*, occurring exclusively in the *cannabis* plant; *endogenous*, produced in humans and other animals; and *synthetic cannabinoids*, which are chemically similar compounds produced in a laboratory. The mechanisms of action for most of these molecules are still not fully understood and evidence exists that at least some of them do not bind strongly to the well known cannabinoid receptors but rather may exert their effects, at least in part, through other

* This work was supported by São Paulo State Research Foundation Grants 03/00231-0 (to A. L. B. A.), 99/03387-4, and 06/00182-8 (to I. P.) and 98/14138-2 (Centro de Biotecnologia Molecular Estrutural), and National Institutes of Health Grants RO1 DA13691 and U19 AI056362 (to R. B. Z.). The costs of publication of this article were defrayed in part by the payment of page charges. This article must therefore be hereby marked "*advertisement*" in accordance with 18 U.S.C. Section 1734 solely to indicate this fact.
The atomic coordinates and structure factors (code 2OM9) have been deposited in the Protein Data Bank, Research Collaboratory for Structural Bioinformatics, Rutgers University, New Brunswick, NJ (http://www.rcsb.org/).
[1] Current address: C3-137 Veterinary Medical Center, Cornell University, Ithaca, NY 14853. To whom correspondence may be addressed: Tel.: 607-253-3653; Fax: 607-253-3659; E-mail: ala48@cornell.edu.
[2] To whom correspondence may be addressed. Tel.: 55-16-3373-9846; Fax: 55-16-3373-9881; E-mail: richard@if.sc.usp.br.
[3] The abbreviations used are: PPAR, peroxisome proliferator-activated receptor; LBD, ligand binding domain; TZD, thiazolidinediones; AJA, ajulemic acid.

yet-to-be discovered receptors. Some of these are already beginning to surface.

Due to the observed functional similarity between effects mediated by PPAR and those activated by this class of compound, cannabinoids are believed to somehow regulate PPARγ isotype functions in living organisms, in a CB1-/CB2-independent manner. For example, naturally occurring Δ^9-tetrahydrocannabinol (THC) stimulates time-dependent vasorelaxation and adipocyte differentiation through activation of PPARγ (14). Furthermore, two endogenous cannabinoids, anandamide and 2-arachidonyl glycerol, have been shown to induce, respectively, the differentiation of 3T3-L1 pre-adipocytes and the modulation of interleukin-2 expression via PPARγ (15, 16). Ajulemic acid (AJA), a synthetic THC analog, on the other hand induces potent analgesic and anti-inflammatory activity without the psychotropic effects of THC, in an event also mediated by PPARγ (17, 18).

AJA (also known as CT-3, IP-751, or 1′,1′-dimethylheptyl-Δ^8-tetrahydrocannabinol-11-oic acid) was originally designed based on observations of the metabolic transformations of THC using the metabolite THC-11-oic acid as a template (19–23). AJA suppresses neuropathic pain in humans and prevents joint tissue injury in rat models of inflammatory arthritis (24–26). In all cases, these effects are observed without producing the motor side effects associated with THC.

In this work we present the crystal structure of the LBD of PPARγ in complex with ajulemic acid, determined at 2.8-Å resolution. The refined model presents a ligand binding mode that is largely determined by the ω-loop and that does not involve the C-terminal helix H12, as has been typically observed for other partial agonists. Molecules of AJA were also bound to the protein surface, more specifically at the recognition/binding site for co-regulator proteins. Structural comparisons between our model and others available from the PDB provide clues to the understanding of the structural basis of one of the principal mechanistic mysteries surrounding this family of nuclear receptors: the nature of partial agonism. AJA based studies demonstrate that both naturally occurring and synthetic cannabinoids may represent novel lead compounds for the development of analogs with potent anti-inflammatory activity and potentially high therapeutic index, because cannabinoids generally present minimal toxicity.

EXPERIMENTAL PROCEDURES

Expression and Purification of the Human PPARγ-LBD—The LBD fragment of the human PPARγ (residues Leu^{204}-Tyr^{477}) amplified from a cDNA library from human fetal brain tissue (Invitrogen), was cloned into the pET28a(+) plasmid (Novagen) using the NdeI and XhoI restriction sites and subsequently used to transform *Escherichia coli* BL21(DE3) cells (Stratagene). Protein expression was induced by the addition of 1 mM isopropyl 1-thio-β-D-galactopyranoside when the cell culture reached an optical density of 1 and left for 3 h at 23 °C. Cells were collected by rapid centrifugation and resuspended in 50 mM Tris/HCl, pH 8.0, 100 mM NaCl containing 1 mM phenylmethylsulfonyl fluoride. Cell lysis was performed using lysozyme treatment followed by sonication. After collecting the soluble fraction, the protein product was isolated in a single purification step by immobilized metal affinity chromatography using the Co^{2+}-charged resin TALON (BD Biosciences), previously equilibrated with the running buffer 50 mM NaCl, 25 mM Tris-HCl, pH 8.0. The PPARγ-LBD bearing a His tag fused to its N terminus was eluted stepwise using running buffer to which up to 200 mM imidazole had been added. After purification, 5 mM dithiothreitol was added to the buffer. The His tag was removed by digestion with bovine thrombin (Sigma) and the protein concentrated to about 300 μM (protein concentrations were determined with the Bradford assay), without the need for removal of the liberated His tag or excess imidazole. AJA, in 100% ethanol at a concentration of 100 mM, was added to the concentrated protein solution at a 10:1 molar excess, and incubated on ice for 1 h prior to crystallization trials.

Crystallization and Data Collection/Processing—Crystallization experiments were performed at 10 °C using the conventional hanging drop vapor diffusion technique. Drops were made by mixing equal parts (2.5 μl each) of protein and well solution, containing 4 M sodium formate. Before data collection at cryogenic temperature (100 K), crystals were soaked with a cryoprotectant solution containing 15% ethylene glycol and 4 M sodium formate and flash frozen. A substantially complete x-ray diffraction data set to 2.8-Å resolution was obtained using Cu-Kα radiation from a Rigaku ultraX 18 rotating-anode home source, equipped with Osmic focusing mirrors and measured on a Mar345 dtb image plate detector. Data were integrated and scaled using the HKL200 suite (27).

Phasing and Model Refinement—The first set of phases was obtained by the molecular replacement technique as implemented in the program Molrep (28), searching for six monomers in the asymmetric unit, as predicted from the Matthews coefficient (29). A monomer of a human PPARγ-LBD *apo* structure was used as the search model (PDB code 1PRG (6)). Straightforward solutions were found for only four monomers in the asymmetric unit, indicating a high solvent content in the crystal (about 68%). Rigid body and simulated annealing refinement were performed using CNS (30), followed by subsequent cycles of positional and *B* factor refinement carried out with REFMAC (31). Real space refinement, including Fourier electron density map inspection, was performed with Coot (32). Non-crystallographic symmetry restraints were used during refinement up until the final stages of TLS refinement. Solvent water molecules, treated as oxygen atoms, were added using the appropriate Coot routine. During the model refinement, the inspection of Fourier difference maps indicated the presence of very strong non-protein electron densities (over 3σ in height) in each monomer of the asymmetric unit both inside the canonical ligand binding cavity and also within the co-regulator recognition pit. Due to their size and shape they were both readily identified as ajulemic acid molecules and subsequently refined as such.

The overall stereochemical quality of the final model and the agreements between model and experimental data were assessed by both the program PROCHECK (33) and the appropriate Coot routines. Comparative B factor analysis across all known PPARγ structures was performed by normalizing the original *B* factors within a range from 0 to 1 (dividing every value by the highest for each model), to minimize the effects

of different resolutions, refinement protocols, and crystal packing.

RESULTS AND DISCUSSION

Overall Structure—After extensive optimization, the best co-crystals of human PPARγ-LBD bound to ajulemic acid were obtained at 10 °C in the presence of 4 M sodium formate. After 4 days growth, plate-like crystals appeared with dimensions of ~0.6 × 0.5 × 0.05 mm, which belonged to space group P1. The Matthew coefficient initially suggested the possibility of six monomers in the asymmetric unit (V_M = 2.57 Å^3/Da with 52.2% solvent) but the results of molecular replacement and subsequent refinement showed unambiguously the presence of only four, corresponding to a V_M of 3.86 Å^3/Da and a solvent content of 68.2%.

The final model was refined until convergence of the reliability indices to 21.7 (R_{factor}) and 26.7% (R_{free}), and consists of four copies of the LBD monomer in the asymmetric unit, 8 molecules of AJA and 213 water molecules. The structure of AJA and its relationship to other cannabinoids is shown in Fig. 1. There are two AJA molecules bound per monomer of LBD, one inside the ligand binding pocket and a second at the protein surface, occupying the co-regulator (external) binding site, as shown in Fig. 2*a*. In the final structure, 91.5% of residues were in the most favorable regions of the Ramachandran plot, 7.9% in additionally allowed regions, and the remaining 0.6% in generously allowed regions. Data collection, refinement, and quality parameters as well as the statistics for the final model are summarized in Table 1.

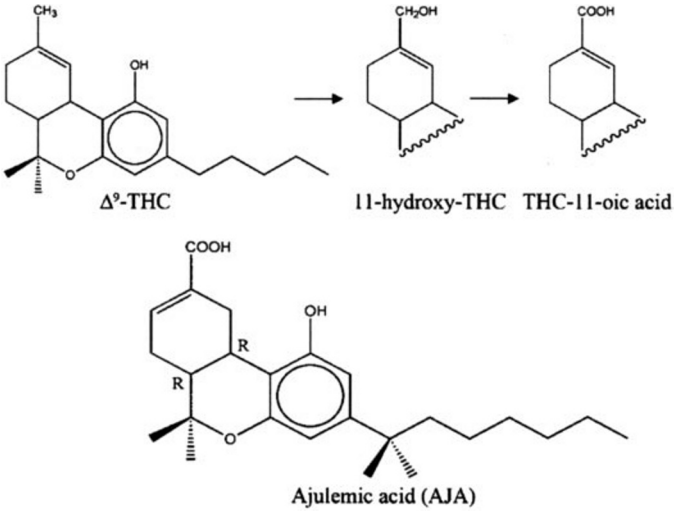

FIGURE 1. **The major pathway of metabolism for THC and the chemical structure of ajulemic acid.** Synthetic modification of the Δ^9-THC metabolite THC-11-oic acid through replacement of the *n*-pentyl side chain with a dimethylheptyl group led to ajulemic acid (*AJA*, $C_{25}H_{36}O_4$).

The best refinement results were reached by using elevated non-crystallographic symmetry weights in a pairwise fashion with chain A coupled to chain C and chain B coupled to chain D, up to the end of the refinement. This was justified mainly by the successful modeling of two regions, between residues Thr^{238} and Lys^{244} and residues Pro^{269} and Lys^{275}, which were observable in the first set of chains (A and C), but were missing in the second (chains B and D). The root mean square deviation, calculated by LSQMAN (34), after superposing all C_α atoms between the two sets of monomers, was 0.46 Å (with a maximum deviation of 1.97 Å). The root mean square deviations between chains A and C and between chains B and D were about 0.08 Å due to the strongly enforced non-crystallographic symmetry. All four LBD monomers present the canonical fold for this family of nuclear receptors, consisting of 12 α-helices (H1 to H12) roughly organized into three layers, as first described by Nolte *et al.* (6).

Protein-protein interfaces that arise as a result of crystal packing were analyzed with the PISA server (35). Monomers share at most 470 Å^2 of hidden surface area in a 2-fold symmetric interface that relates chain A to chain B and also chain C to chain D. This interface is mediated by the binding of two AJA molecules to the external site (Fig. 2*b*) and these have been excluded from the surface area calculations. According to the default criteria used by PISA, about 20 residues from each monomer are involved in the interface, including the formation of two sets of hydrogen bonds: two contacts between residues Gln^{294} (chain A/C) and Gln^{294} (chain B/D) at a separation of about 2.8 Å, and a second between residues Gln^{271} (chain A/C) and Asn^{308} (chain B/D), at a distance of 3.15 Å. Each AJA molecule adds about a further 100 Å^2 to the monomer-monomer interaction surface, increasing the overall interface from 470 to 670 Å^2. Other observed monomer-monomer contacts are only small in area (down to about 70 Å^2) probably due to the relatively high solvent content of the crystal.

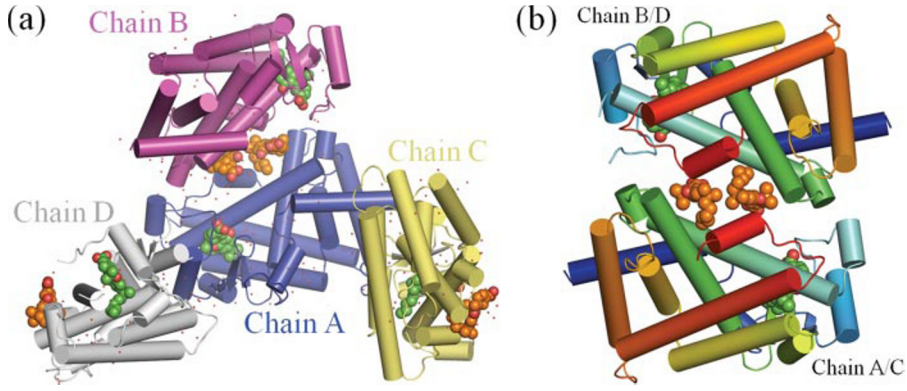

FIGURE 2. **Overall structure of the LBD portion of human PPARγ in complex with AJA.** *a*, asymmetric unit content of the P1 crystal, containing 4 molecules of PPAR-LBD, each associated with 2 molecules of ajulemic acid (represented in *spheres*): those represented in *green* are bound to the canonical ligand binding pocket and those in *orange* are bound to the monomer, in the co-regulator recognition pit. *b*, dimer of LBD induced by the presence of AJA bound in the co-activator binding site (*orange spheres*), with LBD molecules rainbow-colored from N- (in *blue*) to C-terminal (*red*).

AJA Bound to the Ligand Binding Pocket—Ligand binding modes are observed to be similar in all copies of the LBD and therefore interactions will be described in terms of a generic model. Ajulemic acid occupies about 30% of the total volume of the PPARγ T-shaped ligand binding cavity (~1300 A^3, according to

TABLE 1
Data collection parameters and structure refinement statistics
Values in parentheses are for the outer resolution shells.

Data collection	
Space group	P1
Cell parameters	a = 62.3 Å, b = 78.1 Å, c = 104.2 Å, α = 100.1°, β = 106.4°, γ = 90.0°
Resolution range (Å)	30.0–2.8 (2.9–2.8)
Unique reflections	42,977 (4,149)
Redundancy	1.8 (1.6)
R_{symm} (%)	9.0 (30.6)
Completeness (%)	93.8 (90.1)
$I/\sigma(I)$	8.1 (1.8)
B factor from Wilson plot (Å^2)	61.6
Monomers/AU	4
Solvent content (%)	68
Matthews coefficient (A^3/Da)	3.86
Refinement	
R_{factor}/R_{free} (%)	21.7/26.7
Average B factor/root mean square deviation (Å^2)	
Main chain (1060 residues)	39.0/0.74
Side chain (962 residues)	39.3/1.20
Ajulemic acid (8 molecules)	33.4/2.07
Solvent (213 molecules)	32.1/6.67
Root mean square deviation from standard geometries (Å)	
Bond length (Å)	0.012
Bond angles (°)	1.586
Ramachandran plot	
Most favored (%)	91.5
Allowed (%)	7.9
Generously allowed (%)	0.6

Nolte *et al.* (6)). AJA is accommodated inside the pocket by wrapping around helix H3, and is surrounded by helices H4, H7, H8, and β-strand 3. There are no direct contacts with H12, as already observed in other *holo* structures of complexes with partial agonists, such as the complexes with PA-082 (2FVJ (36)) and GW0072 (4PRG, (37)). Nevertheless, H12 is folded over the binding pocket in the "active" conformation (see below).

Polar contacts are made mainly with the final portion of the *ω-loop*, where the acidic head group of AJA interacts with the main chain nitrogen of residues Lys^{256} and His^{266}. Hydrogen bonds from this moiety are also observed with the side chain of Ser^{342} (present in the β-strand 3) and a water molecule. Both the oxygen present in the central ring of AJA and the hydroxyl group in the aromatic ring make no contacts with either protein atoms or solvent molecules.

Non-polar contacts are observed along the full extension of the AJA molecule right out to the end of its aliphatic tail. These contacts start at the ω-loop of the protein, and extend all the way through the ligand binding pocket. Residues involved in these interactions include Phe^{264} (part of the ω-loop), Ile^{281}, Phe^{282}, Gly^{284}, Cys^{285}, Val^{339}, Ile^{341}, Met^{348}, Leu^{353}, and Leu^{356}. Details are depicted in Fig. 3, *a* and *b*.

The presence of AJA inside the ligand binding pocket appears to induce a unique conformation of the ω-loop, when compared with other *apo* and *holo* structures. Along with direct interactions with AJA, the conformation adopted by the loop seems to be in part stabilized by π-stacking between the side chains of residues His^{266} from the ω-loop itself and Phe^{287} (from H4), and unusually, a single-turn 3_{10}-helix is formed at the end of the ω-loop by residues Leu^{270}, Gln^{271}, and Glu^{272}.

Structural Basis of AJA Selectivity for PPAR Isotype γ—Liu and co-workers (17) have shown, by both reporter gene and *in vitro* assays, that AJA binds directly and selectively to mouse PPARγ at pharmacological concentrations, without affecting the activation of isotypes α and δ (both from mouse) when compared with vehicle and type-specific ligand treatment. The sequence identity shared between the isotypes for the LBD portion is about 65%. By combining structural information together with sequence alignments, the basis for this selectivity can be readily assigned and furthermore, can be generalized to

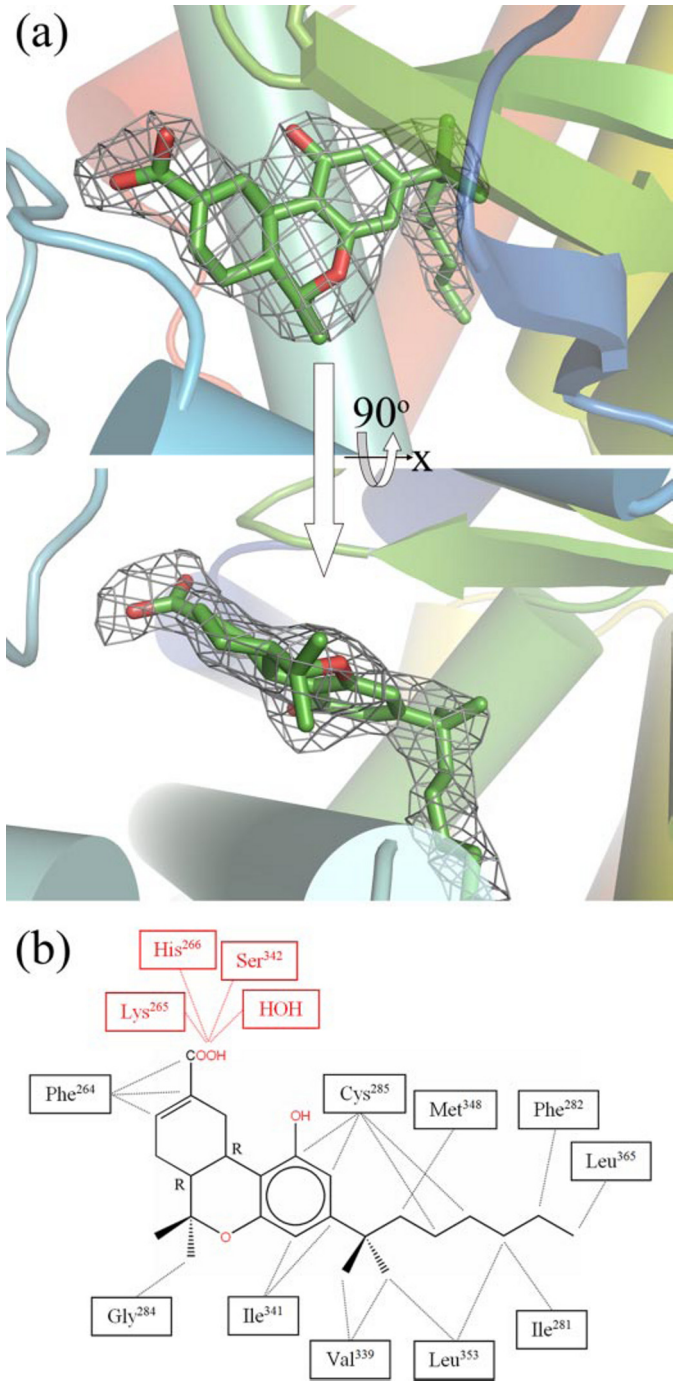

FIGURE 3. **AJA bound inside the ligand binding pocket.** *a*, omit Fourier difference map (3σ, α_{calc}), calculated from the final coordinates, excluding the ajulemic acid molecule, shown in two perpendicular views. *b*, interactions of ajulemic acid with the PPAR-LBD binding pocket. Polar (*red*) and non-polar (*black*) interactions were defined by PyMol.

human PPARs. In the following description the numbering used is that for PPARγ.

Key residues in the surroundings of the ω-loop seem to play a major role in determining selectivity. In the model described here, the side chain of Phe^{264} (present within the ω-loop) makes extensive non-polar contacts with AJA. Substitution of this residue by an alanine, as observed in both human and mouse PPARα, would be expected to eliminate such contacts. On the other hand, the presence of the even bulkier tryptophan side chain in this position in PPARδ causes a narrowing of the pocket toward the ω-loop impeding the entrance of the terminal ring of AJA. Steric hindrance might also be a consequence of the substitution of Gly^{284} (in PPARγ) by cysteine and arginine residues in PPARα and PPARδ, respectively. Finally, Ser^{342} makes a hydrogen bond to the AJA acidic head group via its side chain and this is substituted by alanine in other PPAR isotypes, from both organisms.

It is also worth noting that the residues that share the π-stacking arrangement (His^{266} and Phe^{287}) associated with the unusual conformation of the ω-loop described here and that appears to be associated with AJA binding, are not conserved in the remaining isotypes. Substitutions of hydrophobic residues in the inner part of the binding pocket seems not be of great importance for subtype selection.

AJA Bound to the Co-regulator (External) Binding Site—Unexpectedly, ajulemic acid molecules were also found interacting with the external surface of the protein, more specifically to the co-regulator recognition/binding pit and stabilized mostly by hydrophobic contacts. A single polar contact is found between one oxygen atom from the carboxylic acid group of AJA and the side chain of Lys^{301}. One side of the cyclic moiety of AJA makes non-polar interactions all the way down to the hydrophobic pocket, which is occupied by the aliphatic heptil side chain of AJA. This pocket is formed by residues Ile^{296}, Thr^{297}, Lys^{319}, Leu^{318}, Val^{322}, and Ile^{472}.

The other side of the AJA ring system interacts with the second LBD molecule, which is related by the pseudodyad axis. The monomer:monomer 2-fold symmetry relationship is broken by small changes in some side chains. At this interface, the ajulemic acid makes two polar contacts with the symmetry-related LBD monomer: one hydrogen bond between one of the oxygens of the carboxylic acid group of the ligand and the side chains of residues Gln^{294} and another between the oxygen of the intermediate ring of AJA and the imidazole group of His^{466}. An exception is found in chains A and C, where the contact between AJA and Gln^{294} is missing (schematically represented in Fig. 4*a*).

To check whether AJA induces LBD dimerization in solution, via interaction with the protein surface, or is just a requirement for crystal growth (acting effectively as a crystallization additive), we performed a gel filtration analysis of PPAR-LBD in the presence of different ligands (data not shown). Experiments were carried using a Superdex-75 HR 10/30 analytical gel filtration column (GE Healthcare) and the TZD analog ciglitazone (Cayman Chemical) as a positive control. The presence of either AJA or ciglitazone, even at ×10 molar excess did not alter the elution volume of the protein from the column demonstrating it to be monomeric under all conditions tested, as observed for the *apo* state. Therefore, we conclude that the binding of AJA to the external site is essential for crystal growth, but not sufficient to alter the oligomeric state of the protein when in solution. The presence of crystallization additives (non-ionic detergents) bound to the co-activator binding site has also been described in the crystal structures of PPARδ-LBD (2AWH and 2B50 (38)) and RARγ (1FCY (39–40). However, this is the first time that an agonist has been described bound to both functional sites of the receptor, the canonical ligand binding cavity and the co-regulator binding pit.

Co-activators and peptides derived therefrom interact with nuclear receptors in an agonist-dependent manner through a conserved L*XX*LL motif (*X* being any amino acid), also known as the "NR box." This co-activator domain is correctly orientated with respect to the receptor by the presence of a "charge clamp" on the latter, formed by residues Lys^{301} (within H3) and Glu^{471} (in H12 (6, 41, 42)). By superposing our structure on those that contain the co-activator peptide in complex with the LBD, it becomes clear that the dimethylheptyl side chain of AJA mimics the side chain of the first leucine residue of the L*XX*LL motif and the dimethyl group in the middle ring of AJA is spatially related to the last leucine in the "NR box" motif (as illustrated in Fig. 4*b*). The acidic group of AJA makes polar contacts with Lys^{301}.

Recent studies by Arnold and co-workers (43) exploit this region in the search for alternative methods to regulate gene transcription modulated by the thyroid hormone receptor. Based on high-throughput screening using an *in vitro* fluorescence polarization assay, they measured the ability of small molecules to selective inhibit the interaction between the thyroid receptor-LBD and its co-activator, SRC2, in an isotype-dependent manner. Such compounds, described as a new class of antagonists, bind to the co-regulator binding cleft only after administration of agonists that are known to induce the closed conformation of H12, such as the natural hormone T3.

Comparative Analysis and Hints toward Partial Agonism in PPARγ—Currently, little is known about the molecular mechanisms that lead to partial *versus* full agonism in nuclear receptors. However, recent crystallographic and solution studies have provided clues toward a common mechanism. It has been shown by NMR that the *apo* form of the PPARγ–LBD can best be described as an equilibrium ensemble rather than a single stable conformation and that ligand binding shifts this conformational equilibrium to a state that favors co-activator recruitment. This suggests that the surroundings of H12 (whose conformation is critical for the formation of the co-activator binding surface) are the focus of this dynamic behavior (44, 45).

By gathering all the available crystal structures of the PPARγ–LBD, a similar analysis can be made. LBD structures of the isotype γ, determined by x-ray crystallography and currently deposited in the PDB (as of June 2006) exist in both *apo* and *holo* forms. In the latter case the ligand may be either a full or partial agonist. Overall, 34 crystallographically independent LBD structures were compared by treating the subunits independently, when more than one LBD molecule is present in the asymmetric unit. Besides monomers A and B of the AJA complex described here, the following molecules were included: 1K74 (2), 1I7I (3), 2PRG (6), 3PRG (7), 2FVJ (36), 4PRG (37),

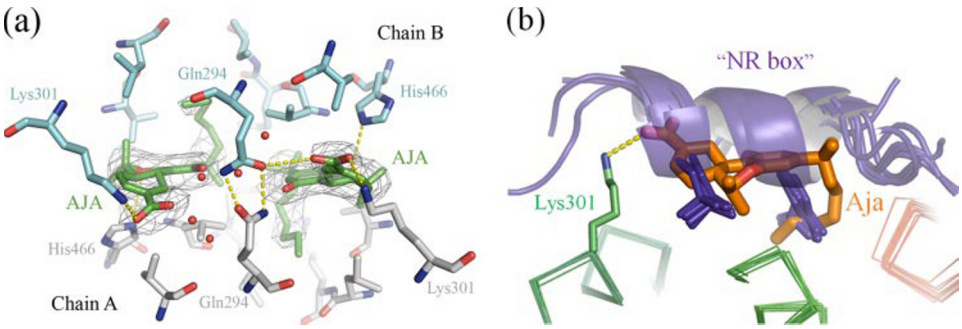

FIGURE 4. **AJA bound in the co-regulator binding site.** *a*, LBD-LBD interface meditated by the presence of AJA interacting with the co-regulator recognition pit. Omit Fourier difference map (3σ, α_{calc}) is shown for the ajulemic acid molecules. *b*, superposition of a single monomer of the LBD·AJA complex with structures determined in the presence of co-activator peptides (that form the interacting region called the NR-box). Aliphatic chains of AJA mimics essential leucine side chain interactions between the peptide and the hydrophobic pit and polar contact between the acidic group of AJA and Lys[301] (part of the "charge clamp") are represented.

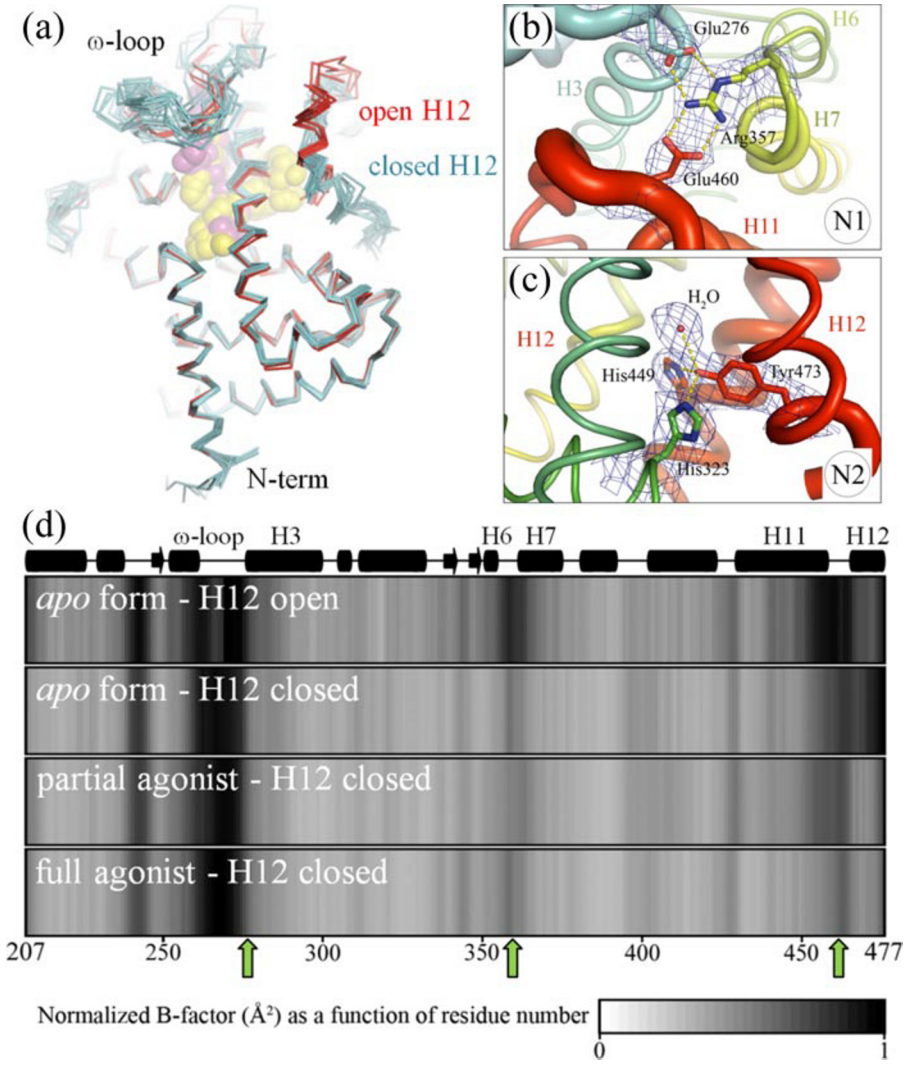

FIGURE 5. **Structural comparison between the crystallographic models of PPARγ-LBD.** *a*, overall comparison of 32 monomers suggests that major conformational differences are found in the region of the ω-loop that connects H2′ to H3 and at H12. According to this pattern, the models were divided in two groups: active, with H12 in the closed conformation (*cyan*), and inactive (*red*). Ligands are show with spheres: *yellow* for full agonists and *pink* for partial agonists. *b* and *c*, $2F_{obs} - F_{calc}$ Fourier map (contoured at 1σ) of residues involved in hydrogen bond networks N1 and N2, respectively. The *thickness* of the schematic representation is directly proportional to the temperature factor of the region. *d*, average normalized *B* factor for each group of molecules showing the overall variation of the temperature factor of the LBD according to the presence or absence of ligands. *Green arrows* indicate the position of residues present in N1. LSQMAN (34) and O2D (62) were used to produce *d*.

1FM6 and 1FM9 (46), 2G0G and 2G0H (47), 1PRG and 1KNU (48), 1NYX (49), 1RDT (50), 1WM0 (51), 1ZGY (52), 2F4B (53), and 1ZEO (54).

Overall comparison reveals minor variations between the 32 monomers and indicates that the principal changes occur: (i) within a range of 20 residues, from position 260 to 279, which are part of the C-terminal region of the ω-loop (between H2′ and H3), and extending into the N-terminal region of H3; (ii) within the loop that connects H6 to H7; and (iii) at the end of H11. Furthermore, two distinct conformations are found for H12: one dominant (80% of all monomers), where H12 is found to be occluding the ligand binding pocket and exposing the co-activator interaction pit, referred to as the "active" conformation, and another (the remaining 20%), referred to as "inactive," where H12 is slightly protruding from the LBD, as can be seen in Fig. 5*a*.

In the "active" group, *holo* structures formed by interaction with either full agonists (14 examples) or partial agonists (8 examples), as well as *apo* structures (4 examples), can be found. On the other hand, in the "inactive" group, only *apo* molecules (4 examples) and partial agonist complexes (2 examples) are present. Therefore, notwithstanding the limited statistics, a trend can still be observed in which 100, 80, and 50%, respectively, of full agonist complexes, partial agonist complexes, and *apo* structures adopt the "active" conformation. It is worth mentioning that in all cases in which H12 is in the inactive state, it is always observed to adopt the same open conformation interacting with the co-regulator binding pit of a crystallographically related mate. This is interpreted as being a lattice-induced stabilization of an intrinsically mobile structure and probably does not reflect the true flexible nature of H12 in inactive structures in solution.

A closer look at members of both groups reveals the details involved

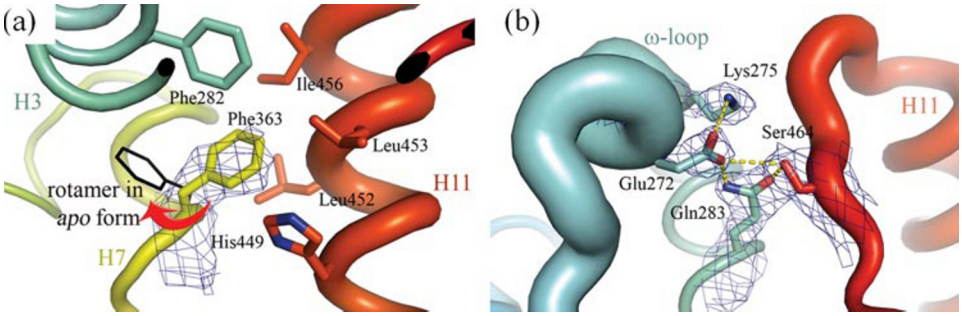

FIGURE 6. **Additional contacts induced by the presence of AJA that may help in reducing intrinsic LBD dynamics.** $2F_{obs} - F_{calc}$ Fourier map (1σ) of key residues in the surroundings of H11 that may help further stabilize N1 and N2 leading to weak but significant transcriptional AF-2 activity compared with *apo* forms: *a*, flipping in the side chain of Phe^{363} due to the presence of partial agonists, and *b*, hydrogen bonds linking the ω-loop to the loop that connects H11 and H12.

in the conformational change leading from one state to another. Monomers in the "active" group share a common network of salt bridges between the side chains of residues Glu^{276} (present toward the end of the ω-loop), Arg^{357} (from the loop between H6 and H7), and Glu^{460} (in the loop between H11 and H12), which will be referred to as N1. It is also a common feature of the *apo* and partial agonist active structures described here, that Tyr^{473} (in H12) makes polar contacts with His^{323} (in H5) and His^{449} (H11), helping to stabilize H12 in the closed (active) conformation. This second set of H-bonds will be called N2. Monomer A of the crystal structure described in this article is used to generically depict N1 and N2, which are shown in Fig. 5, *b* and *c*. In the case of the full agonist structures the interaction between Tyr^{473} and His^{449} is broken due to steric hindrance and polar contacts generated directly between the ligand itself and the aforementioned residues. All members of the "inactive" group lack both of hydrogen bond networks N1 and N2 as described above.

Considering only *apo* structures, examples of which occur in both groups, an analysis of the normalized B-factor distribution throughout the LBD, shows that the formation of N1 seems to play an important role in limiting the mobility of three regions that are major sources of movement: the N-terminal portion of H3, the loop between H6 and H7, and the end of H11, as can be seen in Fig. 5*d*. This is presumably a consequence of the fact that each of these regions provides one of the canonical charged residues that make up the N1 network.

What then, is the nature of partial agonism? The dynamic behavior of the *apo* LBD in solution means that N1 and N2 networks are able to form even in the absence of a ligand but are anticipated to be less stable due to the lack of the direct interactions made between full agonists and H12 (via Tyr^{473}). Partial agonists, on the other hand would be expected to stabilize N1 and N2 networks (and therefore the active conformation) to an extent that is intermediate between an *apo* structure and a full agonist complex. This is consistent with the fact that none of the partial agonists (PA-082 (36), GW0072 (37), 2 pyrazol-5-ylbenzenesulfonamide derivatives (47), and AJA) make direct polar contacts with H12 or residues involved in co-activator recruitment. Rather, they are in majority found closer to the ω-loop branch of the T-shaped ligand binding pocket, making direct contact with the loop itself. The pyrazol-5-yl-benzenesulfonamide derivatives make hydrophobic contact with residues at the end of the loop that connects H11 and H12 and early residues in H12.

If the majority of the partial agonists do not interact with H12, how do they influence N1 and N2 to stabilize the active conformation better than an *apo* structure and thereby lead to weak but significant transcriptional AF-2 activity? The AJA complex reveals two possible mechanisms, one of which may be generic to partial agonists and the other more specific. The generic mechanism involves the side chain of Phe^{363} on H7, which adopts a conformation that is dominant to all partial agonist complexes. Normally Phe^{363} occupies the opposite part of the ligand binding cavity but due to steric hindrance with partial agonists (which, different from full agonists, occupy this region of the cavity) it is forced to flip by 90–180° and insert into a hydrophobic pocket formed by Leu^{452}, Leu^{453}, Ile^{456} (all from H11), His^{449}, and Phe^{282}. This has the effect of stabilizing the interaction between H7 and H11 and favoring the formation of N1 (via the participation of Glu^{460} from the H11/H12 loop) and subsequently N2 (via Tyr^{473}) on H12 itself (Fig. 6*a*).

The more specific mechanism, which may not be applicable to all partial agonists, involves the formation of a further network of hydrogen bonds involving Glu^{272}, Lys^{275}, Gln^{283}, and Ser^{464}, the latter found in the loop connecting H11 and H12 (Fig. 6*b*). This network is generated as a consequence of strong hydrogen bonds formed by the carboxylic acid of AJA with Lys^{265} and His^{266}, which distorts the C-terminal region of the ω-loop. The consequence is to stabilize the loop between H11 and H12, via Ser^{464}, thus once again favoring the N1 network.

A further aspect of a model that purports to explain partial agonism is that it should be in agreement with the proposal that a partial agonist must also allow co-repressor recruitment by the receptor thereby being able to act as either an AF-2 agonist or antagonist depending on cellular context (55, 56). Currently, there are no crystallographic structures of the PPARγ-LBD in complex with antagonists. However, a hypothetical scheme can be envisioned based on the LBD from PPARα with which PPARγ shares about 65% identity and for which a similar N1 network is observed (Fig. 7). The ternary complex between PPARα-LBD, the antagonist GW6471, and a SMRT co-repressor motif (PDB code 1KKQ (57)) shows the antagonist to make direct non-polar contacts with residues in H12, such as Leu^{456}, leading to a shift in Tyr^{464} (the homologue of Tyr^{473} in PPARγ) and to breakage of the N2 network. As a consequence, H12 undergoes a rigid body shift toward the N terminus of H3, leaving space to accommodate co-repressor binding.

Assuming that the behavior of PPARα can be taken as a model for co-repressor binding to PPARγ (as has been seen for the case of co-activators), then it is necessary that the binding of a partial agonist does not completely restrict the conformation adopted by H12. The observation made here that the crystal structures of partial agonist complexes present both the active

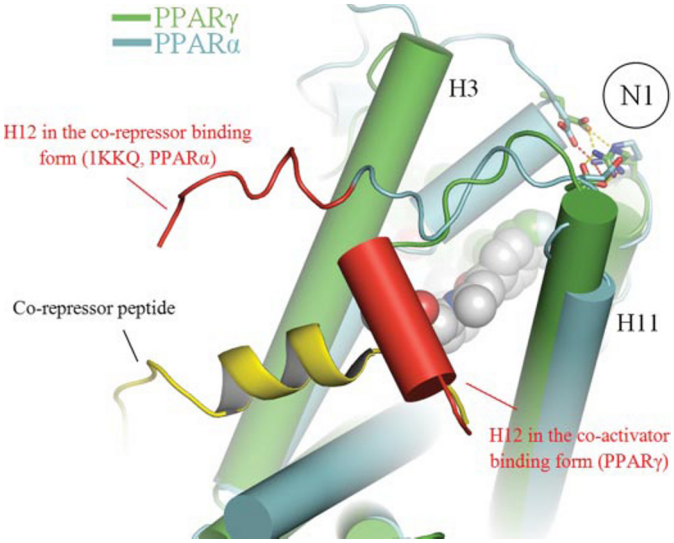

FIGURE 7. **Conformational changes to H12 in PPARα-LBD, induced as a consequence of the presence of antagonist.** H12 is able to undergo a significant conformational change to accommodate co-regulators. The weaker stabilization of H12 (via N1 and N2) in the case of partial agonists still allows H12 to assume the conformation suitable for co-repressor recruitment, as seen in PPARα. This helix H12 could presumably undergo a rigid body shift between the agonist- and antagonist-induced positions and the equilibrium would be dictated by the intracellular concentration of co-activators and co-repressors.

and inactive conformations for H12, and that the partial agonists do not stabilize the closed conformation of H12 directly, is consistent with this notion. The weaker stabilization of H12 (via N1 and N2) in the case of partial agonists still allows H12 to assume the conformation suitable for co-repressor recruitment, as seen in PPARα. This helix could presumably swing between the agonist- and antagonist-induced positions and the equilibrium would be dictated by the intracellular concentration of co-activators and co-repressors.

One exception is the crystal structure of the PPARγ-LBD in complex with the full agonist 2-BABA BVT.13 (1WM0 (51)), where neither direct nor indirect interaction with H12, are observed, and yet this compound activates the receptor to levels comparable with the TZD analogs. Therefore other factors contributing to partial activity cannot be ruled out.

In summary, the model proposed here is that partial agonism could be reached by enhancing the stability of the closed conformation of H12 over and above that seen in the random fluctuations of the *apo* structures. This occurs by binding to the branch of the ligand binding cavity closer to the ω-loop and thereby inducing conformational changes in key residues in the surroundings of H12, decreasing the overall dynamic behavior of the LBD, yet without restricting the flexibility of the latter to the point where co-repressor recruitment is impeded.

Conclusions—We have described the crystallographic model of the PPARγ-LBD portion of the human PPAR bound to a synthetic cannabinoid, ajulemic acid, determined at 2.8-Å resolution. This is the first structural evidence that THC analogs may bind to receptors other than CB1 and CB2, in agreement with the available biochemical and pharmacological data. Furthermore, to our knowledge, it is the first crystal structure of a cannabinoid bound to a protein receptor.

It has been shown that AJA induces moderate activation of AF-2 function, and consistently with the data provided by other structures of LBDs bound to partial agonists, AJA is bound to the ω-loop branch of the ligand binding pocket, not making any direct contact with H12. The pattern of interactions found for AJA, as well as other partial agonists, inside the bulky pocket induces an increase in the number of contacts between major dynamic regions of the LBD, such as the N terminus of H3, the loop joining H6 to H7 and H11. As a consequence, H12 would be expected to be restricted to oscillate back and forth between the co-activator and co-repressor states, depending on the cellular context.

Recent reviews suggest that partial agonism, might be the most effective strategy to fight metabolic diseases, for example, diabetes type 2, by stimulating insulin sensitivity without promoting adipogenesis (58, 59). The model described here may serve as an initial guide in the rational design of molecules that can regulate partial or minimum activity of the isotype γ of the PPAR family of receptors. Furthermore, because of the high degree of structural similarity between nuclear receptors, it is possible that conclusions reached here may be extended to other members of the family, such as the estrogen receptor (60) and the liver X receptor (61), for which partial agonists have been described.

AJA was also found in the co-regulator binding pocket, acting as a crystallization additive, in an interaction that is favored by the presence of its long aliphatic chain that lodges in the hydrophobic co-activator binding pit in a manner already observed for other fortuitous ligands. Analysis of these interactions may help rationalize the design of small ligands that bind specifically to this region, as an alternative method to regulate transcription initiation by nuclear receptors. In summary, our results show that AJA, as well as other THC analogs, in presenting specific binding together with minimal toxicity and good bioavailability may provide useful novel templates for rational drug design aimed at PPARγ regulation.

Acknowledgments—Graphical representations of the coordinate file were prepared by using PyMOL. We thank Dr. Zbigniew Dauter for help with crystallographic data processing.

REFERENCES

1. Michalik, L., and Wahli, W. (1999) *Curr. Opin. Biotech.* **10,** 564–570
2. Xu, H. E., Lambert, M. H., Montana, V. G., Plunket, K. D., Moore, L. B., Collins, J. L., Oplinger, J. A., Kliewer, S. A., Gampe, R. T., McKee, D. D., Moore, J. T., and Willson, T. M. (2001) *Proc. Natl. Acad. Sci. U. S. A.* **98,** 13919–13924
3. Cronet, P. J., Petersen, F., Folmer, R., Blomberg, N., Sjoblom, K., Karlsson, U., Lindstedt, E. L., and Bamberg, K. (2001) *Structure* **9,** 699–706
4. Alarcon de la Lastra, C., Sanchez-Fidalgo, S., Villegas, I., and Motilva, V. (2004) *Curr. Pharm. Des.* **10,** 3505–3524
5. Sung, B., Park, S., Yu, B. P., and Chung, H. Y. (2004) *J. Gerontol. A Biol. Sci. Med. Sci.* **59,** 997–1006
6. Nolte, R. T., Wisely, G. B., Westin, S., Cobb, J. E., Lambert, M. H., Kurokawa, R., Rosenfeld, M. G., Willson, T. M., Glass, C. K., and Milburn, M. V. (1998) *Nature* **395,** 137–143
7. Uppenberg, J., Svensson, C., Jaki, M., Bertilsson, G., Jendeberg, L., and Berskentam, A. (1998) *J. Biol. Chem.* **272,** 31108–31112
8. Forman, B. M., Tontonoz, P., Chen, J., Brun, R. P., Spiegelman, B. M., and Evans, R. M. (1995) *Cell* **83,** 803–812

9. Kliewer, S. A., Forman, B. M., Blumberg, B., Ong, E. S., Borgmeyer, U., Mangelsdorf, D. J., Umesono, K., and Evans, R. M. (1994) *Proc. Natl. Acad. Sci. U. S. A.* **91,** 7355–7359
10. Nagy, L., Tontonoz, P., Alvarez, J. G., Chen, H., and Evans, R. M. (1998) *Cell* **93,** 229–240
11. Lehmann, J. M., Moore, L. B., Smith-Oliver, T. A., Wilkison, W. O., Willson, T. M., and Kliewer, S. A. (1995) *J. Biol. Chem.* **270,** 12953–12956
12. Willson, T. M., Cobb, J. E., Cowan, D. J., Wiethe, R. W., Correa, I. D., Prakash, S. R., Beck, K. D., Moore, L. B., Kliewer, S. A., and Lehmann, J. M. (1996) *J. Med. Chem.* **39,** 665–668
13. Cobb, J. E., Blanchard, S. G., Boswell, E. G., Brown, K. K., Charifson, P. S., Cooper, J. P., Collins, J. L., Dezube, M., Henke, B. R., Hull-Ryde, E. A., Lake, D. H., Lenhard, J. M., Oliver, W., Jr., Oplinger, J., Pentti, M., Parks, D. J., Plunket, K. D., and Tong, W. Q. (1998) *J. Med. Chem.* **41,** 5055–5069
14. O'Sullivan, S. E., Tarling, E. J., Bennett, A. J., Kendall, D. A., and Randall, M. D. (2005) *Biochem. Biophys. Res. Commun.* **337,** 824–831
15. Bouaboula, M., Hilairet, S., Marchand, J., Fajas, L., Le Fur, G., and Casellas, P. (2006) *Eur. J. Pharmacol.* **517,** 174–181
16. Rockwell, C. E., Snider, N. T., Thompson, J. T., Vanden-Heuvel, J. P., and Kaminski, N. E. (2006) *Mol. Pharmacaol.* **70,** 101–111
17. Liu, J., Li, H., Burstein, S. H., Zurier, R. B., and Chen, J. D. (2003) *Mol. Pharmacol.* **63,** 983–992
18. Burstein, S. H., Karst, M., Schneider, U., and Zurier, R. B. (2004) *Life Sci.* **75,** 1513–1522
19. Burstein, S. H., Hunter, S. A., Latham, V., and Renzulli, L. (1987) *Experientia* (*Basel*) **43,** 402–403
20. Burstein, S. H., and Shoupe, T. S. (1981) *Drug Metab. Dispos.* **9,** 94–96
21. Burstein, S. H., Rosenfeld, J., and Wittstruck, T. (1972) *Science* **176,** 422–423
22. Burstein, S. H., and Kupfer, D. (1971) *Chem. Biol. Interact.* **3,** 316
23. Burstein, S. H., Menezes, F., Williamson, E., and Mechoulam, R. (1970) *Nature* **225,** 87–88
24. Dyson, A., Peacock, M., Chen, A., Courade, J. P., Yagoob, M., Groarke, A., Brain, C., Loong, Y., and Fox, A. (2005) *Pain* **116,** 129–137
25. Mitchell, V. A., Aslan, S., Safaei, R., and Vaughan, C. W. (2005) *Neurosci. Lett.* **382,** 231–235
26. Karst, M., Salim, K., Burstein, S., Conrad, I., Hoy, L., and Schneider, U. (2003) *J. Am. Med. Assoc.* **290,** 1757–1762
27. Otwinowski, Z., and Minor, W. (1997) *Methods Enzymol.* **276,** 307–326
28. Vagin, A., and Teplyakov, A. (1997) *J. Appl. Crystallogr.* **30,** 1022–1025
29. Matthews, B. M. (1968) *J. Mol. Biol.* **33,** 491–497
30. Brunger, A. T., Adams, P. D., Clore, G. M., DeLano, W. L., Gros, P., Grosse-Kunstleve, R. W., Jiang, J. S., Kuszewski, J., Nilges, M., Pannu, N. S., Read, R. J., Rice, L. M., Simonson, T., and Warren, G. (1998) *Acta Crystallogr. Sect. D Biol. Crystallogr.* **54,** 905–921
31. Murshudov, G. N., Vagin, A. A., and Dodson, E. J. (1997) *Acta Crystallogr. D Biol. Crystallogr.* **53,** 240–255
32. Emsley, P., and Cowtan, K. (2004) *Acta Crystallogr. Sec. D Biol. Crystallogr.* **60,** 2126–2132
33. Laskowski, R. A., MacArthur, M. W., Moss, D. S., and Thornton, J. M. (1993) *J. Appl. Crystallogr.* **26,** 283–291
34. Kleywegt, G. J., and Jones, T. A. (1994) *CCP4/ESF-EACBM Newsletter Protein Crystallogr.* **31,** 9–14
35. Krissinel, E., and Henrick, K. (2005) in *CompLife 2005*, *LNBI 3695* (Berthold, M. R., Glen, R., Diederichs, K., Kohlbacher, O., and Fischer, I., eds) pp. 163–174, Springer-Verlag, Berlin
36. Burgermeister, E., Schnoebelen, A., Flament, A., Benz, J., Stihle, M., Gsell, B., Rufer, A., Ruf, A., Kuhn, B., Maerki, H. P., Mizrahi, J., Sebokova, E., Niesor, E., and Meyer, M. (2006) *Mol. Endocrinol.* **20,** 809–830
37. Oberfield, J. L., Collins, J. L., Holmes, C. P., Goreham, D. M., Cooper, J. P., Cobb, J. E., Lenhard, J. M., Hull-Ryde, E. A., Mohr, C. E., Blanchard, S. G., Parks, D. J., Moore, L. B., Lehmann, J. M., Plunket, K., Miller, A. B., Milburn, M. V., Kliewer, S. A., and Willson, T. M. (1999) *Proc. Natl. Acad. Sci. U. S. A.* **96,** 6102–6106
38. Fyffe, S. A., Alphey, M. S., Buetow, L., Smith, T. K., Ferguson, M. A., Sørensen, M. D., Björkling, F., and Hunter, W. N. (2006) *J. Mol. Biol.* **356,** 1005–1013
39. Klaholz, B. P., Mitschler, A., and Moras, D. (2000) *J. Mol. Biol.* **302,** 155–170
40. Klaholz, B. P., and Moras, D. (2000) *Acta Crystallograp. Sect. D Biol. Crystallogr.* **56,** 933–935
41. Heery, D. M., Kalkhoven, E., Hoare, S., and Parker, M. G. (1997) *Nature* **387,** 733–736
42. Torchia, J., Rose, D. W., Inostroza, J., Kamei, Y., Westin, S., Glass, C. K., and Rosenfeld, M. G. (1997) *Nature* **387,** 677–784
43. Arnold, L. A., Estebanez-Perpina, E., Togashi, M., Jouravel, N., Shelat, A., McReynolds, A. C., Mar, E., Nguyen, P., Baxter, J. D., Fletterick, R. J., Webb, P., and Guy, R. K. (2005) *J. Biol. Chem.* **280,** 43048–43055
44. Johnson, B. A., Wilson, E. M., Li, Y., Moller, D. E., Smith, R. G., and Zhou, G. (2000) *J. Mol. Biol.* **298,** 187–194
45. Hamuro, Y., Coales, S. J., Morrow, J. A., Molnar, K. S., Tuske, S. J., Southern, M. R., and Griffin, P. R. (2006) *Protein Sci.* **15,** 1883–1892
46. Gampe, R. T., Montana, G. T., Lambert, M. H., Miller, A. B., Bledsoe, R. K., Milburn, M. V., Kliewer, S. A., Wilson, T. M., and Xu, H. E. (2000) *Mol. Cell* **5,** 545–555
47. Lu, I. L., Huang, C. F., Peng, Y. H., Lin, Y. T., Hsieh, H. P., Chen, C. T., Lien, T. W., Lee, H. J., Mahindroo, N., Prakash, E., Yueh, A., Chen, H. Y., Goparaju, C. M., Chen, X., Liao, C. C., Chao, Y. S., Hsu, J. T., and Wu, S. Y. (2006) *J. Med. Chem.* **49,** 2703–2712
48. Sauerberg, P., Pettersson, I., Jeppesen, L., Bury, P. S., Mogensen, J. P., Wassermann, K., Brand, C. L., Sturis, J., Wöldike, H. F., Fleckner, J., Andersen, A. S. T., Mortensen, S. B., Svensson, L. A., Rasmussen, H. B., Lehmann, S. V., Polivka, Z., Sindelar, K., Panajotova, V., Ynddal, L., and Wulff, E. M. (2002) *J. Med. Chem.* **45,** 789–804
49. Ebdrup, S., Pettersson, I., Rasmussen, H. B., Deussen, H. J., Jensen, A. F., Mortensen, S. B., Fleckner, J., Pridal, L., Nygaard, L., and Sauerberg, P. (2003) *J. Med. Chem.* **46,** 1306–1317
50. Haffner, C. D., Lenhard, J. M., Miller, A. B., McDougald, D. L., Dwornik, K., Ittoop, O. R., Gampe, R. T., Xu, E. H., Blanchard, S., Montana, V. G., Consler, T. G., Bledsoe, R. K., Ayscue, A., and Croom, D. (2004) *J. Med. Chem.* **47,** 2010–2029
51. Östberg, T., Svensson, S., Selén, G., Uppenberg, J., Thor, M., Sundbom, M., Sydow-Bäckman, M., Gustavsson, A. L., and Jendeberg, L. (2004) *J. Biol. Chem.* **279,** 41124–41130
52. Li, Y., Choi, M., Suíno, K., Kovach, A., Daugherty, J., Kliewer, S. A., and Xu, H. E. (2005) *Proc. Natl. Acad. Sci. U. S. A.* **102,** 9505–9510
53. Mahindroo, N., Wang, C. C., Liao, C. C., Huang, C. F., Lu, I. L., Lien, T. W., Peng, Y. H., Huang, W. J., Lin, Y. T., Hsu, M. C., Lin, C. H., Tsai, C. H., Hsu, J. T. A., Chen, X., Lyu, P. C., Chao, Y. S., Wu, S. Y., and Hsieh, H. P. (2006) *J. Med. Chem.* **49,** 1212–1216
54. Shi, G. Q., Dropinski, J. F., McKeever, B. M., Xu, S., Becker, J. W., Berger, J. P., MacNaul, K. L., Elbrecht, A., Zhou, G., Doebber, T. W., Wang, P., Chao, Y.-S., Forrest, M., Heck, J. V., Moller, D. E., and Jones, B. A. (2005) *J. Med. Chem.* **48,** 4457–4468
55. Lavinsky, R. M., Jepsen, K., Heinzel, T., Torchia, J., Mullen, T. M., Schiff, R., Del-Rio, A. L., Ricote, M., Ngo, S., Gemsch, J., Hilsenbeck, S. G., Osborne, C. K., Glass, C. K., Rosenfeld, M. G., and Rose, D. W. (1998) *Proc. Natl. Acad. Sci. U. S. A.* **95,** 2920–2925
56. Germain, P., Staels, B., Dacquet, C., Spedding, M., and Laudet, V. (2006) *Pharmacol. Rev.* **58,** 685–704
57. Xu, H. E., Stanley, T. B., Montana, V. G., Lambert, M. H., Shearer, B. G., Cobb, J. E., McKee, D. D., Galardi, C. M., Plunket, K. D., Nolte, R. T., Parks, D. J., Moore, J. T., Kliewer, S. A., Willson, T. M., and Stimmel, J. B. (2002) *Nature* **415,** 815–817
58. Cock, T. A., Houten, S. M., and Auwerx, J. (2004) *EMBO Rep.* **5,** 142–147
59. Knouff, C., and Auwerx, J. (2004) *Endocr. Rev.* **25,** 899–918
60. Pike, A. C. W., Brzozowski, A. M., Hubbard, R. E., Bonn, T., Thorsell, A.-G., Engstrom, O., Ljunggren, J., Gustaffson, J.-A., and Carlquist, M. (1999) *EMBO J.* **18,** 4608–4618
61. Albers, M., Blume, B., Schlueter, T., Wright, M. B., Kober, I., Kremoser, C., Deuschle, U., and Koegl, M. (2006) *J. Biol. Chem.* **281,** 4920–4930
62. Kleywegt, G. J. (1997) *CCP4/ESF-EACBM Newsletter Protein Crystallogr.* **34,** 5–8